Original Article

Ann Colorectal Res 2019;7(4):2-8.

Annals of Colorectal Research

Localisation of Zones of Cancer Detection in Prostate Gland Using Ratio Matrix and Radial Scanning of 2D Trans-rectal Ultrasound Images

Vincent Chukwudi Chijindu[1]*, Chidiebele C. Udeze[1], Mamilus A. Ahaneku[1], Ijeoma J.F. Anarado-Ezika[1], Kennedy Chinedu Okafor[2]

[1]*Department of Electronic Engineering, University of Nigeria, Nsukka, Enugu State, Nigeria*
[2]*Department of Mechatronic Engineering, Federal University of Technology Owerri, Imo State, Nigeria*

***Corresponding authors:**
Vincent Chukwudi Chijindu,
Department of Electronic Engineering, University of Nigeria, Nsukka, Enugu State, Nigeria. **Email:** vincent.chijindu@unn.edu.ng

Received: 26-11-2019
Revised: 11-12-2019
Accepted: 11-12-2019

Abstract

Researchers have continued to proffer various solutions to the challenge of delineating from Trans-rectal ultrasound (TRUS) 2D-images of the prostate the regions of desired property. This paper presents an algorithm that categorises the detected regions suspected to be cancerous, hyper-echoic pixels, in the prostate gland from a 2D Trans-rectal Ultrasound images into three zones. The developed algorithm uses radial scanning of the pixels of the prostate gland image from common seed point both to detect and delineate the suspected cancerous pixels into zones, namely peripheral, transition and central, by applying ratios of the anatomical zones of the prostate gland. Expert knowledge, intensity and gradient features were implemented to delineate regions of interest. MATLAB programming tool was used for creating the codes that implemented the algorithms. Samples of TRUS 2D-images of the prostate for patients with raised PSA values (>10 ng/ml) used in a previous work by Award (2007) were used for testing the algorithm. The test results showed that the algorithm could detect zones of the prostate boundary exhibit image properties for cancer cells and also the percentage of malignancy detected in zones agreed with existing research findings. Comparison of detection results with that of an expert radiologist yielded the following performance parameters; accuracy of 88.55% and sensitivity of 71.65%.

Keywords: Image, Hyper-echoic, Prostate, Localisation, Anatomical, Zones, Segmentation

Please cite this paper as:
Chukwudi Chijindu V, Udeze CC, Ahaneku MA, Anarado-Ezika IJF, Okafor KC. Localisation of Zones of Cancer Detection in Prostate Gland Using Ratio Matrix and Radial Scanning of 2D Trans-rectal Ultrasound Images. *Ann Colorectal Res*. 2019;7(4):2-8. doi: .

Introduction

The second most common cancer reported worldwide for males is prostate cancer. The estimated number of new diagnoses in 2012 was 1.1 million for this condition (1). Prostate cancer is reportedly the most commonly diagnosed cancer in men aside cancers of the skin. Moreover, research shows that about 180,890 new cases of prostate cancer were projected for the US in 2016 (2). Although prostate cancer is less aggressive than numerous other cancers, early diagnosis of occurrence is vital for treatment of this disease due to its widespread tendency. Available treatment has been found to be successful for early stages of the cancer. To detect cancer in early stages, it is necessary for men above 50 years of age to be screened annually (3). Automated segmentation of medical images plays a critical role in medical imaging applications. Its applications are in different areas such as diagnosis, localization of pathology, study of anatomical structure, treatment planning, and computer-integrated surgery. The fact that the anatomical structures of the human body are very complex and vary from person to person has resulted in medical image segmentation remaining a hard problem (4). Over the last few years of intellectual discourse and research, the problem of prostate segmentation for delineating boundaries and volumes has received considerable attention (5-7). Different segmentation techniques have been applied by different researchers. Among these techniques are the edge-detection, graph-searching, deformable models, geodesic active contours, thresholding, classification, clustering, region growing, split and merge, atlas-guided, artificial neural network, and watershed techniques (8). Ladak et al. (9) presented a method that uses the deformable contour model, also called the discrete dynamic contour (DDC) (10). To initialize the method, the user is required to select only four points. These points are applied to a cubic interpolation function and shape information to estimate the outline of the prostate. Careful initialization of contour by marking points on the prostate boundary is however key to the success of their approach.

Yang et al. (11) proposed an automatic segmentation algorithm that uses atlas registration with statistical priors on texture of image. Gabor features that were specific to patients obtained from the atlas database were used in training the kernel support vector machines (KSVMs). Zhan et al. (12) proposed the use of a deformable contour for automating the extraction of prostate boundary from trans-rectal ultrasound (TRUS) images. This involves matching of both shape and texture statistical properties to segment the prostate. Subsequently, a set of Gabor-support vector machines (G-SVM) are applied on different patches of the model surface. The G-SVM is then trained using adaptive method to obtain the texture priors of TRUS images that help in classifying tissues to be prostate or non-prostate within the zones of the prostate boundary. Akbari et al. (13) developed an algorithm that involves texture information, intensity profiles, and statistical shape. The sub-regions of the prostate gland are subjected to a set of waves (W-SVMs). Finally, the result obtained is fine-tuned using intensity profiles subject to the detected boundaries. Award (14) proposed a technique that uses expert knowledge and gradient vector flow (GVF) deformable contour to both segment the prostate boundary and detect suspected cancerous regions within the prostate gland. These previous works used techniques that require a lot of computation time and training data. Support vector machines and its variants have a disadvantage of long run time to achieve the needed convergence. For detection of specific regions of interest, the mentioned techniques will require even more computation time; hence, there is a need for a fast and robust method. The new technique compliments the propositions of Wu et al. (15) and Eskandari et al. (16) for delineating prostate gland by implementing experts' knowledge while radially scanning pixel features to detect suspected cancerous tissues. The new algorithm emphasizes detection of hyper-echoic pixels within the region of the prostate gland before delineating and categorizing them into zones using anatomical ratios. Consequently, the gland image is divided into sixteen sections fewer than in (16). In addition, the following expert knowledge was implemented: Cancerous cells are not scattered, but occur in clusters; cancer is not likely to occur along the edges of the gland, but rather occurs within the gland zones (14). The benefit of the fewer sections is reduced processing time giving rise to a fast detection algorithm. The pixel intensity ranges that represent hyper-echoic intensity are 0 to 55 for dark images and 0 to 50 for light images (on a grayscale image intensity range of 0 to 255) (8).

Materials and Methods

The basic materials needed for the execution of this research consisted of the following:

i) Software environment: The implementation of this work required MATLAB version 7.5 or higher running on WINDOWS 7 or higher.

ii) Hardware environment : The hardware requirement for the implementation of this work included a computer with the following specifications:

* Processor: 2.0GHz, 64-bit Operating System or above.
* Installed Memory (RAM): 2.00 Gigabytes or above.
* Hard Disk: 200 Gigabytes or above.

iii) Samples of digitized trans-rectal ultrasound 2D images of the prostate gland. Samples of online images used in a previous work by Awad in 2007 (14) were downloaded and stored in memory as JPEG (.jpg) format digital images using Microsoft Photo

Viewer to review and resize the image accordingly. We note that other digital image formats were considered but JPEG format was chosen because it occupies less memory and is amenable to grey level conversion for image analysis and processing required for the algorithm. The digital graphics image was thus captured in .jpg format. These were brought into the MATLAB program working memory using a Read command as (M x N) array matrix. A typical image was in gray level; the maximum sample value of 255 and minimum sample value of 0 were utilized. The maximum value of 255 represented points of highest intensity (white or very bright), whereas the value of 0 represented points of lowest intensity (black or very dark).

The methods adopted to realize the objectives of the research are described in the proceeding sections.

Method of Detecting Suspected Cancerous Tissues of Prostate Gland Region

In order to automatically extract the prostate gland and detect suspected cancerous sites or tissues from trans-rectal ultrasound 2D-images, a four stage algorithm shown in Figure 1 is described. The first stage of the proposed segmentation algorithm is preparing the image by enhancement using sequential sticks algorithm. This stage ensures reduction of noises, especially speckle noise, which affect TRUS images. The second stage uses the segmentation algorithm described in (16) to build and store the coordinates of the boundary of the prostate gland as well as a centre point (8). Additionally, a lookup table was built using the anatomical zones ratio for pixel coordinates lying within the boundary of the prostate gland. The third stage detects the hyper-echoic pixels within the stored boundaries of the prostate gland using some prior and expert knowledge, and categorizes the pixels detected into zones using a lookup table developed from the anatomical zones ratio for the gland boundary in the image. This stage was comprised of three steps. First, it processes each of the sector (scanning along the

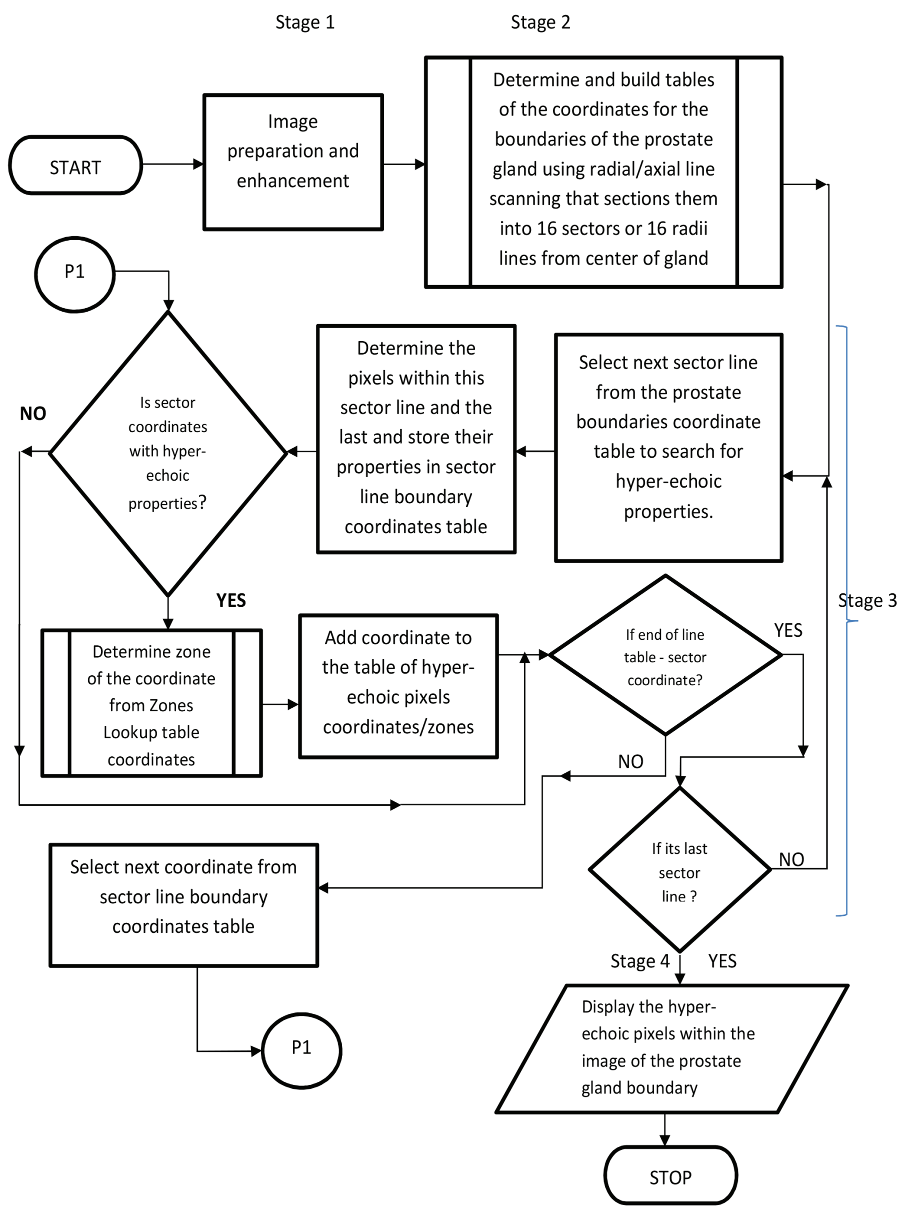

Figure 1: Flowchart of prostate cancer detection and localization by zones algorithm.

radii/axes) boundaries for pixels within it and stores their properties in a sector line boundary coordinates table. Secondly, it checks the table for hyper-echoic properties by applying the prior knowledge. Finally, it searches the anatomical zones lookup table for the coordinates of the detected pixel and stores it for further analysis. The last stage is for analysing and displaying of the hyper-echoic pixels within the image of the prostate gland.

Method of Localizing Zones of Detected Suspected Cancerous Tissues of Prostate Gland

The design here uses ratio-based metrics to partition the prostate gland image matrix. It uses the anatomical zone distribution of the prostate gland proposed by McNeal, including the peripheral (65%), central (25%) and transition (10%) zones (4,14). The seed point coordinate was assumed to be about the centre line of the segmented prostate gland. The segment of the prostate image that is likely to contain the prostate gland was split into 16 segments of 22.5 degrees about the seed point centre axis, as shown in Figure 2. The zones shared the segments in a ratio of 7:2:1 for the peripheral-anterior, central, and transition zones, respectively. The peripheral zone occupies approximately 11 segments (* =11.2); the central zone occupies approximately 3 segments (* =3.2); and the transition zone occupies approximately 2 segments (* =1.6).

The transition zone occupies the 2 segments located in the first 22.5 degrees of the first quadrant and the fourth 22.5 degrees of the fourth quadrant of the axis shown in Figure 2. The central zone is next to the right of the transition zone, occupying the next three segments; it includes the next three 22.5 degrees of the first quadrant.

The peripheral-anterior zone occupies the remaining 11 segments spanning 2nd , 3rd and 1st 3, 22.5 degrees of the 4th quadrant of the axis about the seed point within the matrix of the image. These segments were used to determine the row and column limits for the pixel coordinates that would then be stored for the different zones in the lookup table that is generated. Axial locations of the three zones in the image matrix were used to apportion pixel coordinates to the zones. The converted zone matrix identities were stored in tables.

The lookup table was thus created and used to assign a zone identity to the matrix coordinates of the suspected cancerous tissues of a sample prostate gland image by comparing corresponding matrix coordinates. A count was kept for the detected number of pixels that were suspected cancerous for each of the zones, which corresponded to the area of the zone in pixels. The areas accumulated for each zone in a selected sample were also stored as a percentage of the area of suspected cancerous tissues of the prostate gland.

Method of Evaluating the Result of Proposed

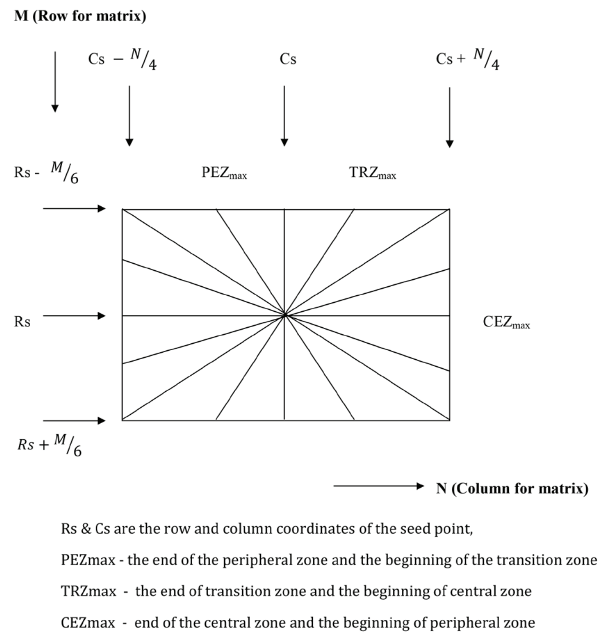

Figure 2: Classifying the matrix of the prostate gland region into 16 segments.

Algorithm

The evaluation of the proposed algorithm uses area-based metrics as described in (8).

The codes for the algorithms were developed using MATLAB programming language. The algorithms were tested with image samples obtained from an earlier work by Award (14).

Results and Discussion

The new algorithm was tested with TRUS 2D image samples of patients who had initial symptoms indicating evidence of prostate cancer at various stages. The result of detections by the new algorithm performed on some of the image samples are shown in Figure 3 (a) to (f). The same image samples were presented to expert radiologists to mark sites in the image suspected to be cancerous and the results obtained are shown in Figure 3 (g) to (l). The two detection results have been presented side by side for comparison.

The results of the new algorithm were evaluated using the area-based metrics outlined in (8). The parameters of sensitivity and accuracy were determined for each image sample.

The average value was determined as well as the standard deviation for the sample results. Average values for these parameters were determined to measure the performance of the new algorithm. From the summary result obtained in the table, the algorithm achieved an accuracy of 84.17% and sensitivity of 78.49%, with standard deviation of 13.84 and 13.68, respectively (8). The new algorithm is simple and does not involve complex and cumbersome computations. The algorithm executes fast and has performance that is highly comparable to existing ones. However, the algorithm fails to detect

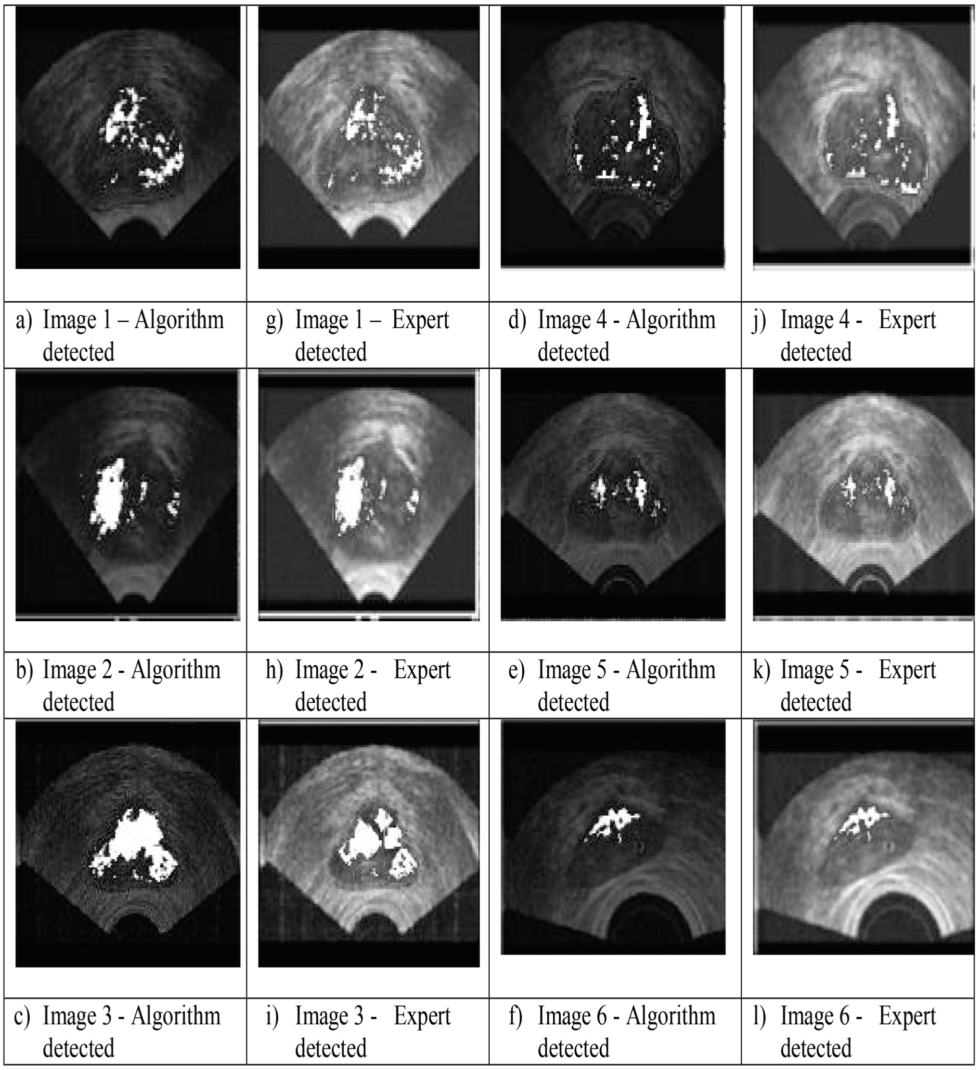

Figure 3: TRUS 2D prostate images samples a) to f) with detected suspected cancer sites marked by new algorithm and g) to l) with detected suspected cancer sites in same samples marked by expert radiologist (8)

gland boundaries where there are tissues that show distinct higher intensities like tissues outside the gland region. This accounts for the low sensitivity value and high standard deviation recorded.

The accuracy value of 84.17% implies that for every detection result by the algorithm, it was about 80% certain (almost certainly true) that the patient with the prostate gland image was likely to have cancer cells in the regions identified. It was also interpreted to mean that the result obtained by the system at any given time for any image sample was almost certainly true.

The algorithm for partitioning the matrix of a sample of prostate image was implemented and the look up table was used to section the detected image into zones. The areas of the zones represented as a percentage of the detected pixels in suspected cancerous tissues for some samples both for expert and algorithmic detection were computed, and the results were represented in a graphical form to pictorially depict the relationship between the algorithm and expert detection results as shown in Figures 4 to 6.

The graph in Figure 4 shows that the pattern of detection in the peripheral zone for both the proposed algorithm and expert opinion follows a close sequence and size. Since more than 70% of cancers originate in this zone, the system guarantees the detection of any such incidence of cancer in the prostate gland tissues.

The graph in Figure 5 reveals that the algorithm's performance in detecting cancer characteristics in the transition zone was close except in four cases, where the expert record higher values. This was partly due to the shortfalls of the zoning algorithm. It can also be due to the maximum malignant dominant intensity value chosen. The result can be improved by adjusting this value upward. Only between 10%-20% of cancers originate in this zone.

Figure 6 reveals that the two curves had similar patterns in the central zone. The system recorded high in two cases while the experts recorded high in five cases. The variance in this case was primarily due to the shortfalls of the zoning algorithm. This result can be improved by adjusting the boundary between the transition and central zones in the zoning algorithm. Only about 5% -10% of cancers originate in this zone.

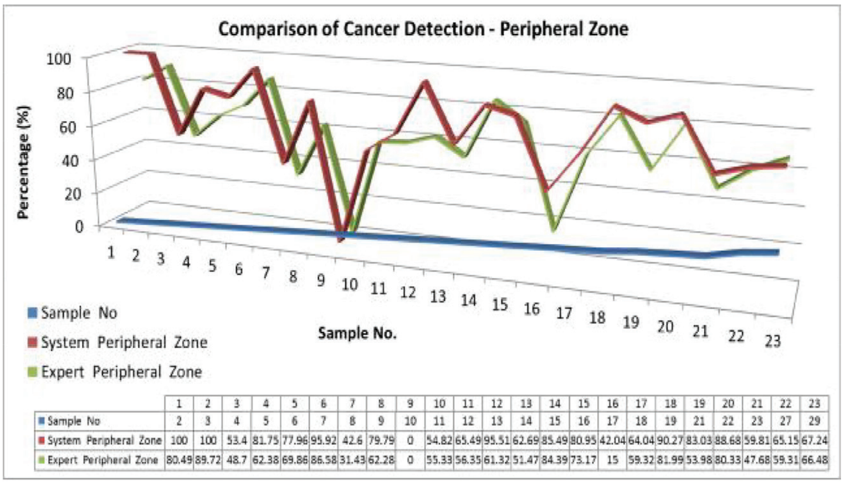

	1	2	3	4	5	6	7	8	9	10	11	12	13	14	15	16	17	18	19	20	21	22	23
Sample No	2	3	4	5	6	7	8	9	10	11	12	13	14	15	16	17	18	19	21	22	23	27	29
System Peripheral Zone	100	100	53.4	81.75	77.96	95.92	42.6	79.79	0	54.82	65.49	95.51	62.69	85.49	80.95	42.04	64.04	90.27	83.03	88.68	59.81	65.15	67.24
Expert Peripheral Zone	80.49	89.72	48.7	62.38	69.86	86.58	31.43	62.28	0	55.33	56.35	61.32	51.47	84.39	73.17	15	59.32	81.99	53.98	80.33	47.68	59.31	66.48

Figure 4: Graphical comparison of cancer detection results between experts and the proposed algorithm: peripheral zone.

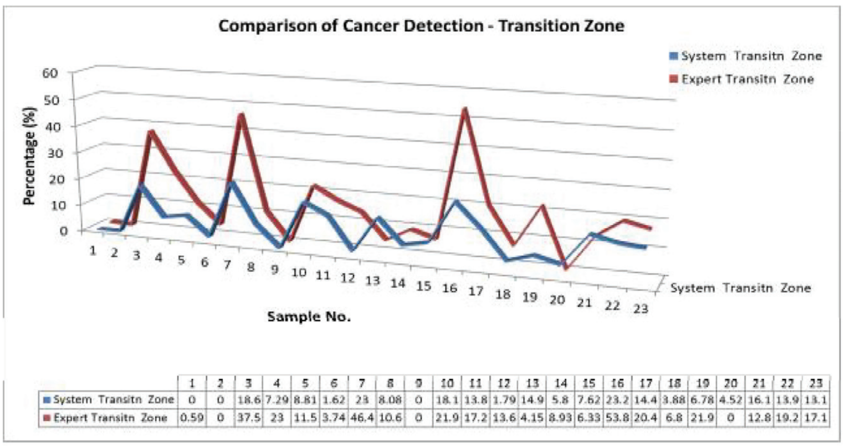

	1	2	3	4	5	6	7	8	9	10	11	12	13	14	15	16	17	18	19	20	21	22	23
System Transitn Zone	0	0	18.6	7.29	8.81	1.62	23	8.08	0	18.1	13.8	1.79	14.9	5.8	7.62	23.2	14.4	3.88	6.78	4.52	16.1	13.9	13.1
Expert Transitn Zone	0.59	0	37.5	23	11.5	3.74	46.4	10.6	0	21.9	17.2	13.6	4.15	8.93	6.33	53.8	20.4	6.8	21.9	0	12.8	19.2	17.1

Figure 5: Graphical comparison of cancer detection results between experts and the proposed algorithm: transition zone.

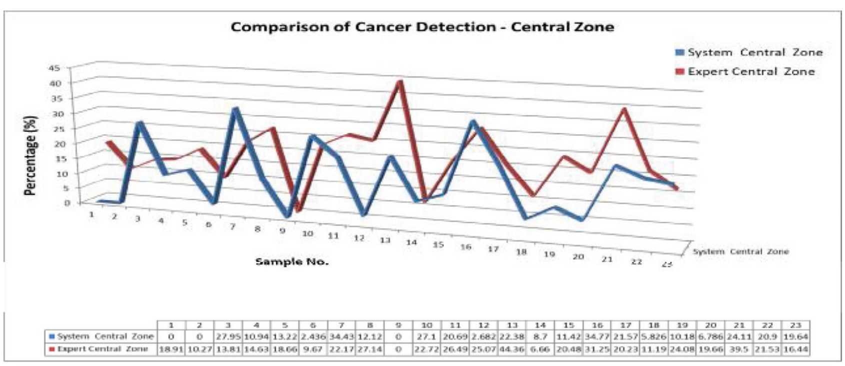

	1	2	3	4	5	6	7	8	9	10	11	12	13	14	15	16	17	18	19	20	21	22	23
System Central Zone	0	0	27.95	10.94	13.22	2.436	34.43	12.12	0	27.1	20.69	2.682	22.38	8.7	11.42	34.77	21.57	5.826	10.18	6.786	24.11	20.9	19.64
Expert Central Zone	18.91	10.27	13.81	14.63	18.66	9.67	22.17	27.14	0	22.72	26.49	25.07	44.36	6.66	20.48	31.25	20.23	11.19	24.08	19.66	39.5	21.53	16.44

Figure 6: Graphical comparison of cancer detection results between experts and the proposed algorithm: central zone.

Conclusion

This work used radial scanning with prior knowledge on image features to detect the prostate gland boundary and subsequently localize into gland zones the suspected cancerous tissues, which were hyper-echoic pixels from an ultrasound 2D image sample of the prostate gland. High accuracy and sensitivity values were achieved by the algorithm for the whole detection when tested with several samples of prostate image.

Localization of detected suspected cancerous regions of the prostate gland was in agreement with the estimated percentages of malignancy in zones of the gland. The results of this work can enhance the expert's ability to localize suspected cancerous regions within the prostate, thereby reducing frequency of biopsies.

Application of the result of this research will go a long way to ensuring early detection of cancer and consequently a reduction in death rates due to undetected cancer. It is believed that the results obtained in this work will assist medical professionals involved in managing prostate disease to provide both routine services and reliable diagnoses.

Further work is recommended to improve on the accuracy and sensitivity of the algorithm, capture the detection in zone s with colors, and compute the accuracy and sensitivity for each of the zones.

Authors' contribution: Authors contributed equally to the manuscript.

Funding/Support: No funding to declare.

Informed Consent: Authors mention that Ethical clearance and consent was obtained from University of Nigeria Teaching Hospital, Ituku-Ozalla Enugu State, Nigeria.

Conflict of Interests: None declared.

References

1. Dabic-Stankovic K, Rajkovic K, Acimovic M, Milosevic N, Stankovic J. A Quantitative Analysis of Two-dimensional Manually Segmented Transrectal Ultrasound Axial Images in Planning High Dose Rate Brachytherapy for Prostate Cancer. Vojnosanit Pregl. 2017; 74(5): 420-427. doi: 10.2298/VSP150901231D
2. Siegel RI, Miller KD, Jemal A. Cancer Statistics, 2016, *CA Cancer J. Clin*. 2016 Jan-Feb; 66(1): 7-30. doi: 10.3322/caac.21332.
3. Yu Y, Cheng J, Li J, Chen W, Chiu B. Automatic Prostate Segmentation from Trans-rectal Ultrasound Images. *2014 IEEE Biomedical Circuits and Systems Conference (BioCAS) Proceedings*. doi:10.1109/BioCAS.2014.6981659
4. Pathak SD, Chalana V, Haynor DR, Kim Y. Edge-Guided Boundary Delineation in Prostate Ultrasound Images. *IEEE Trans Med Imaging*. 2000; 19(12): 543-551.
5. Pham DL, Xu C, Prince JL. Current Methods in Medical Image Segmentation. *Annu. Rev. Biomed. Eng. 2000. 02:315-337*.
6. Liu X, Langer DL, Haider MA, Yang Y, Wemick MN, Yetick IS. Prostate Cancer Segmentation With Simultaneous Estimation of Markov Random Field Parameters and Class. *IEEE Trans Med Imaging. 2009;* 28(6): 906-915.
7. Chiu B. A New Segmentation Algorithm for Prostate Boundary Detection in 2D Ultrasound Images. *Master's thesis, Department of Electrical and Computer Engineering, University of Waterloo*, Waterloo, Ontario, Canada, 2003.
8. Chijindu VC, Udeze CC, Ahaneku MA, Anoliefo EC. Detection of Prostate Cancer Using Radial/ Axial Scanning of 2D Trans-rectal Ultrasound Images. *Bulletin of Electrical Engineering and Informatic*. 2018; 7(2): 222-229. doi: 10.11591/eei.v7i2.727
9. Ladak HM, Mao F, Wang Y, Downey DB, Steinman DA, Fenster A. Prostate Boundary Segmentation from 2D Ultrasound Images. *Med Phys*. 2000 Aug; 27(8): 1777-1788. doi: 10.1118/1.1286722
10. Lobregt S, Viergever MA. A Discrete Dynamic Contour Model. *IEEE Trans Med Imaging,* 1995; 14(1): 12-22.
11. Yang X, Schuster D, Master V, Nieh P, Fenster A, Fei B. Automatic 3D Segmentation of Ultrasound Images Using Atlas Registration and Statistical Texture Prior. *Proc. of SPIE 2011;* 7964:796432-1-8. doi: 10.1117/12.877888
12. Zhan Y, Shen D. Deformable Segmentation of 3D Ultrasound Prostate Images Using Statistical Texture Matching Method. *IEEE Trans Med Imaging*, 2006; 25(3): 256-272.
13. Abari H, Fei B. 3D Ultrasound Image Segmentation Using Wavelet Support Vector Machines. *Med. Phys.* 2012 June; 39(6): 2972-2984. doi: 10.1118/1.4709607
14. Awad JGE. Prostate Segmentation and Regions of Interest Detection in Transrectal Ultrasound Images. *A Doctor of Philosophy Thesis, University of Waterloo, Waterloo*, Ontarion, Canada, 2007.
15. Wu R, Ling KV, Shao W, Ng WS. Registration of Organ Surface with Intra-operative 3D Ultrasound Image Using Genetic Algorithm. *MCCAI 2000; 2878*: 383-390. doi: 10.1007/978-3-540-39899-8_48.
16. Eskandari H, Talebpour A, Tabrizi SH, Nowroozi MR. Development of a Fast Algorithm for Automatic Delineation of Prostate Gland on 2D Ultrasound Images. *Proceedings of the 19th Iranian Conference on Biomedical Engineering (ICBME 2012)*, pp. 313-317, 2012.